International Journal of Medical, Medicine and Health Sciences
ISSN: 2517-9969
Vol:10, No:6, 2016

Analysis of the Internal Mechanical Conditions in the Lower Limb Due to External Loads

Kent Salomonsson, Xuefang Zhao, Sara Kallin

***Abstract*—** Human soft tissue is loaded and deformed by any activity, an effect known as a stress-strain relationship, and is often described by a load and tissue elongation curve. Several advances have been made in the fields of biology and mechanics of soft human tissue. However, there is limited information available on *in vivo* tissue mechanical characteristics and behavior. Confident mechanical properties of human soft tissue cannot be extrapolated from e.g. animal testing. Thus, there is need for non invasive methods to analyze mechanical characteristics of soft human tissue. In the present study, the internal mechanical conditions of the lower limb, which is subject to an external load, is studied by use of the finite element method. A detailed finite element model of the lower limb is made possible by use of MRI scans. Skin, fat, bones, fascia and muscles are represented separately and the material properties for them are obtained from literature. Previous studies have been shown to address macroscopic deformation features, e.g. indentation depth, to a large extent. However, the detail in which the internal anatomical features have been modeled does not reveal the critical internal strains that may induce hypoxia and/or eventual tissue damage. The results of the present study reveals that lumped material models, i.e. averaging of the material properties for the different constituents, does not capture regions of critical strains in contrast to more detailed models.

***Keywords*—**FEM, human soft tissue, indentation, properties.

I. Introduction

HUMAN soft tissue is loaded in almost any situation, resulting in deformation, sometimes the loads even result in tissue damage. Biomechanical understanding of the interaction between the human tissue and the external loading is important in order to decrease the risk of soft tissue damage. Pressure ulcer is a localized damage to the skin and/or underlying soft tissue usually over a bony prominence or related to, e.g., a medical device.

The injury occurs as a result of intense and/or prolonged pressure or pressure in combination with shear as defined by NPUAP (National Pressure Ulcer Advisory Panel) [1]. The necessity of investigations of the internal mechanical conditions due to external loading such as pressure and/or shear is clear while considering an external support design. Finite element analyses (FEA) have been used in many studies to simulate the behavior of soft tissues subjected to external loading, see , e.g., sitting [2], prosthetic sockets e.g. [3], [4], [5], shoulder load carriage [6], calf compression [7]. Boundary conditions, geometries and material models are addressed to develop the FE model of the body segment of interest. The FEA can then be used to predict the stress-strain distribution within the tissues. However, most often these FE models are simplified and the internal strain conditions in the different soft tissues are neglected. Geometries of soft tissues are lumped together, e.g., [2], [3], [5], material properties are not representing the living human tissue, e.g., based on animal studies, [2], [3], [5], [6], and/or isotropic linear or hyperelastic behavior.

Recently more detailed geometries have been used, e.g., [8]. They developed a geometrically detailed model of skin, fat, veins and four muscle compartments in the calf to study the vein vessels deformation due to compressive stockings, and [9] differentiated the muscles of the thigh to identify their Neo-Hookean material parameters during compression. Groves et al. [10] showed that the skin behavior differed between human and swine. Hence, there is still a need of models in which improved representation of soft tissue geometries and material behavior is included.

The aim of current study is to investigate internal mechanical conditions in a section of a human *in vivo* lower leg exposed to a cylindrical indentor while using a geometrically detailed model. The detailed FE model of the leg section is developed with separated soft tissues of skin, fat, bones, fascia and muscles. Comparisons by levels of detailed geometry representations and their impact on internal mechanical conditions of loaded soft tissues are investigated.

II. Method

A. Finite Element Model

The lower limb geometry is acquired from a MRI scan, see Fig. 1, and the resulting FE model of the lower limb considered in this paper is shown in Fig. 2 together with the loading setup. The resolution of the MRI images is approximately 0.5 mm and is considered good enough for the purpose of the present analyses. The fibula and the tibia bones are modeled with both the cortical bone and the bone marrow as separate phases.

The skin, fat, fascia and muscle tissues are modeled using linear continuum elements. The indentor is considered rigid. The strap is modeled using 4-noded shell elements. The complete FE model contains approximately 540000 elements and the commercial finite element software Abaqus 6.14-3 is used as a solver.

B. Boundary Conditions

The boundary conditions are in accordance with the applied boundary conditions that were applied during the in-situ MRI

K. Salomonsson is with the School of Engineering, Jönkoping University, Jönkoping, Sweden (e-mail: kent.salomonsson@ju.se).
X. Zhao is with the School of Engineering, Jönkoping University, Jönkoping, Sweden.
S. Kallin is with the School of Engineering and the School of Health and Welfare, Jönkoping University, Jönkoping, Sweden (e-mail: sara.kallin@ju.se).

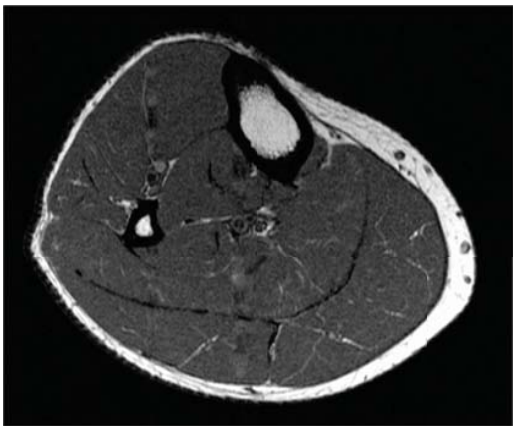

Fig. 1 Sample image from the MRI scan

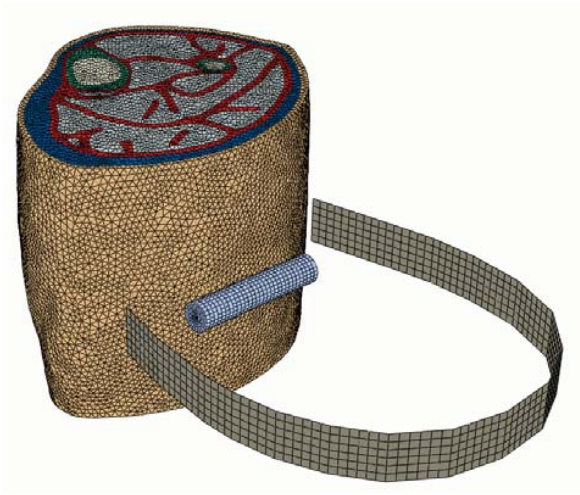

Fig. 2 Finite element setup. The pin is regarded as rigid and the strap is regarded as elastic

experiments, i.e. a cylinder made from a PETG (copolyester of polyethylene terephthalate) thermoplastic is pushed into the soft tissue and then held in place by a plastic strap. The cylinder can be regarded as rigid in the context of soft human tissue and a controlled displacement is applied in the negative z-direction according to Fig. 2. The cylinder is constrained so that it only can move along the z-axis. Symmetry boundary conditions are applied on the lower limb cut surfaces. In order to prevent translation of the FE model, constraints are applied on the tibia and fibula. The controlled displacement of the cylinder pin is 14 mm.

In order to make the strap tight around the lower limb and the cylinder pin, the ends of the strap are controlled to first open up and the translate along the z-axis until the strap makes contact with the cylinder. At this point, the ends of the strap are moved together to surround the lower limb and pin, see Fig. 3.

As can be seen in Fig. 3, the strap pulls the cylinder pin into the lower limb. This was also the procedure during the physical experiment. However, in the physical experiment, the strap was loosened and tightened multiple times in order to

Fig. 3 Loaded FE model with the strap tightend aound the lower limb

make it comfortable for the subject. Thus, as can be seen in Fig. 4. the soft tissues are squeezed between the cylinder and the strap.

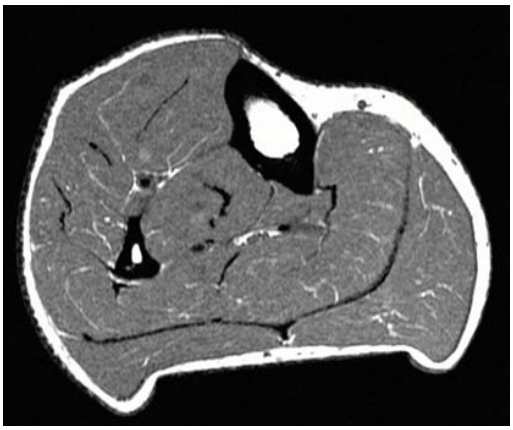

Fig. 4 MRI image of the loaded lower limb

C. Material Data

Soft tissues are usually modeled as either Ogden or polynomial hyperelastic materials, which the chosen approach in this work as well. The Ogden strain energy potential is expressed as,

$$U = \sum_{i=1}^{N} \frac{2\mu_i}{\alpha_i^2}(\lambda_1^{-\alpha_i} + \lambda_2^{-\alpha_i} + \lambda_3^{-\alpha_i} - 3) + \sum_{i=1}^{N} \frac{1}{D_i}(J^{el} - 1)^{2i}$$

where U is the strain energy per unit of reference volume, μ_i, α_i and D_i are material constants, N is the order of the equation, λ_i are the deviatoric principal stretches and J^{el} is the elastic volume ratio. The Ogden model is a function of the principal stretches as opposed to the polynomial strain energy

potential which commonly are functions of deviatoric strain invariants according to,

$$U = \sum_{i+j=1}^{N} C_{ij}(I_1 - 3)^i (I_2 - 3)^j + \sum_{i=1}^{N} \frac{1}{D_i}(J^{el} - 1)^{2i}$$

where C_{ij} contain the material constants and, I_1 and I_2 are the first and second deviatoric strain invariants.

In this work, the skin, the fat, the fascia and the muscle tissues are considered as isotropic. Muscle is modeled as a second order Ogden material with slight compressibility according to [11]. The data used in this model was reported for gluteal muscles. The nonlinear behavior of fat is modeled by adapting the Ogden material model according to [7]. The skin is modeled using the material parameters for a Ogden hyperelastic membrane according to [13]. The material constants of the strain energy function used for muscle, fat and skin are shown in Table I.

TABLE I
MATERIAL CONSTANTS USED IN THE FE MODEL

	[-]	[MPa]	[MPa^{-1}]
Muscle	$\alpha_1 = 1.316$	$\mu_1 = 1.026 \cdot 10^{-2}$	$D_1 = 19.499$
	$\alpha_2 = 18.359$	$\mu_2 = 1.452 \cdot 10^{-7}$	$D_1 = 166.315$
Fat	$\alpha_1 = 0.770$	$\mu_1 = 1.653 \cdot 10^{-2}$	–
Skin	$\alpha_1 = 26.000$	$\mu_1 = 1.0 \cdot 10^{-2}$	–

A polynomial strain energy function according to [12] was used to model the fascia. The material constants of the polynomial strain energy function for this model were: $C_{10} = -222.1$ kPa, $C_{01} = 290.97$ kPa, $C_{20} = -1.1257$ kPa, $C_{11} = 4.7267$ kPa, $C_{02} = 79.602$ kPa.

As mentioned previously, the tibia is considered elastic and isotropic with the Young's modulus 11.8 GPa, which was reported in [14] in the direction perpendicular to axis of tibia. Also, the fibula is assumed to have the same properties as the tibia.

The strap is made of a thermoplastic material with a modulus of elasticity that was set to 200 MPa and Poisson's ratio of 0.40.

III. NUMERICAL RESULTS

By controlling the displacement of a rigid cylinder to compress the lower limb, it was possible to study the internal mechanical strains. A strap made from a generic thermoplastic material was then tightened around the cylinder in order to mimic the physical experiment as good as possible. It is clear, by observing Figs. 5 and 6, that there are differences between the detailed FE model and that of the lumped FE model. Herein, referring to lumped as an averaging of the muscle and fascia material parameters.

A. Fascia

For the individual phases such as the fascia, it is observed in Fig. 7 that it is highly strained. This is due to the relatively soft material parameters as compared to the muscle material parameters. When the lower limb tissues are compressed, it is the softest material that will be compressed the most. In this case it is the fascia. Furthermore, due to the hyperelastic

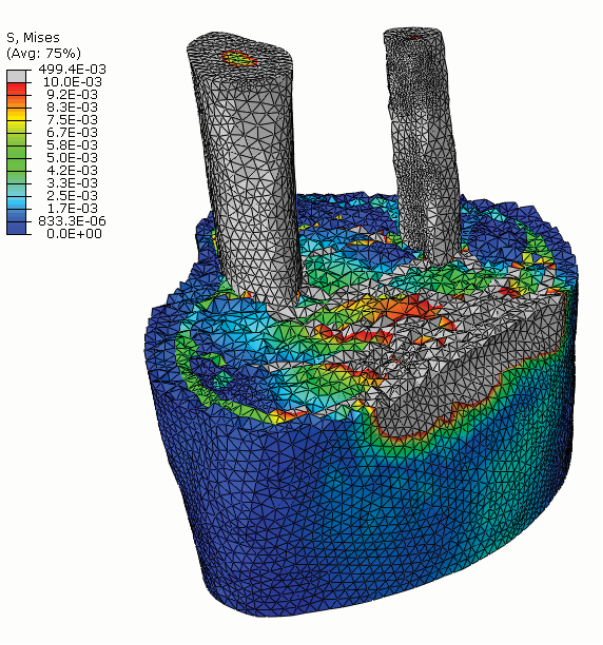

Fig. 5 Contour plot of the detailed FE model showing the von Mises effective stress

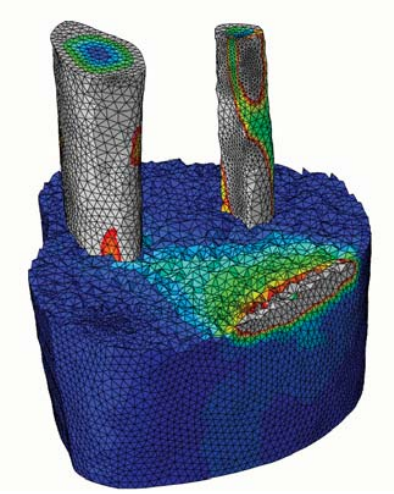

Fig. 6 Contour plot of the lumped FE model showing the von Mises effective stress

properties, it can only be compressed to a certain level which is when it becomes incompressible. At this point, deformation is shifted to the surrounding tissues.

In Fig. 8, it is seen that the deformation is localized. This is an effect of having more volume of the same material properties. The volume that is occupied by the fascia does not compress as much since the muscle and fascia have the same material properties. Thus, there is more volume to compress before the point at which it becomes incompressible is reached.

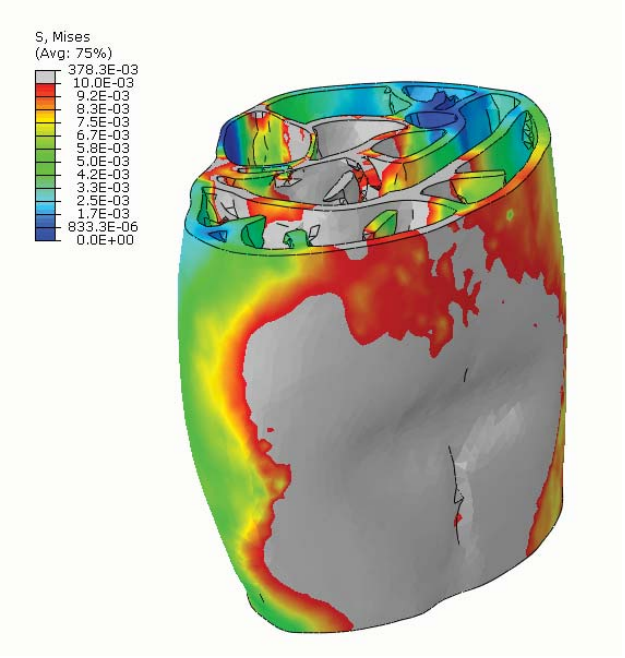

Fig. 7 Contour plot of the fascia tissue from the detailed FE model showing the von Mises effective stress

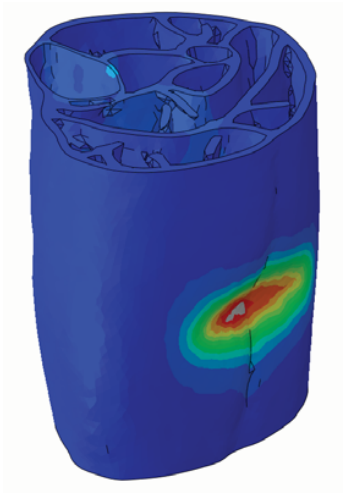

Fig. 8 Contour plot of the fascia tissue from the lumped FE model showing the von Mises effective stress

B. Muscle

The muscle behaves almost the same for the detailed and the lumped model, see Figs. 9 and 10. Given the arguments stated in the fascia section, this is not surprising. It should however be noted that the stresses are slightly higher for the detailed FE model. This is because of the fascia being compressed, i.e. more deformation of the muscle volume since the fascia does not resist the external loads as much.

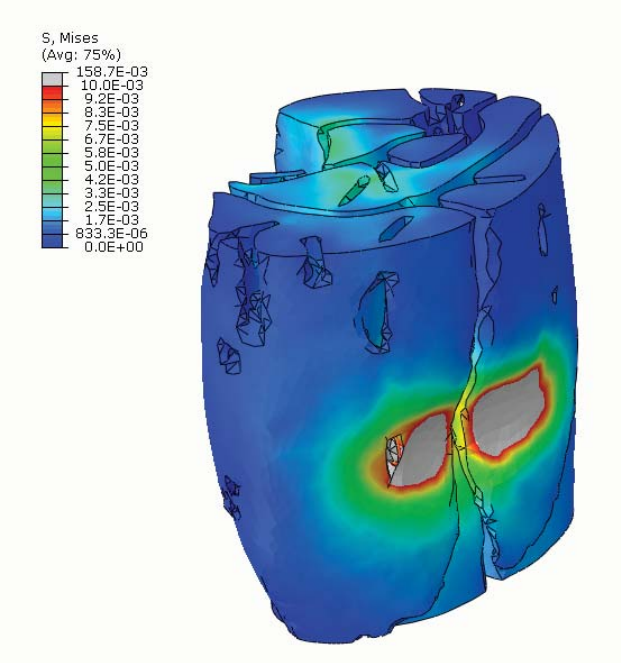

Fig. 9 Contour plot of the muscle tissue from the detailed FE model showing the von Mises effective stress

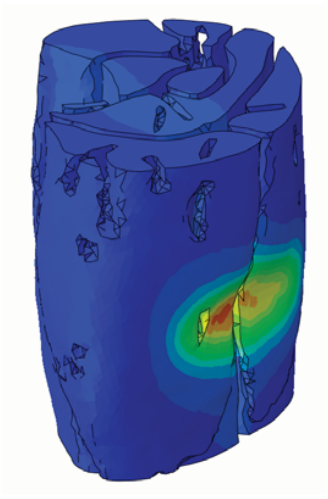

Fig. 10 Contour plot of the muscle tissue from the lumped FE model showing the von Mises effective stress

C. Fat

Much like for the muscle, and for the same reasons, the fat tissue behaves similarly for the detailed model and the lumped model, see Figs. 11 and 12. Slight differences can be seen, such as the almost speckled stress field for the detailed model, see Fig. 11. This is probably due to the shearing of the fascia which is in direct contact with the fat tissue. The fat tissue is also a soft material and two soft material stacked in series during compression will lead to unstable deformation modes.

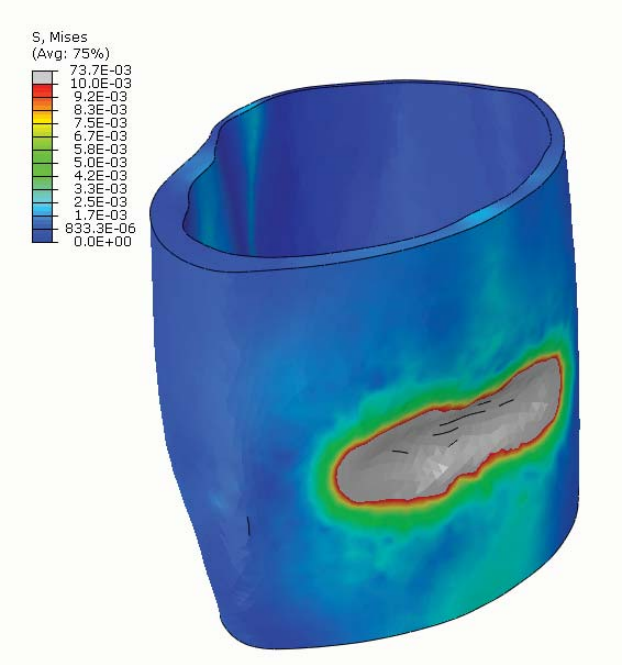

Fig. 11 Contour plot of the fat tissue from the detailed FE model showing the von Mises effective stress

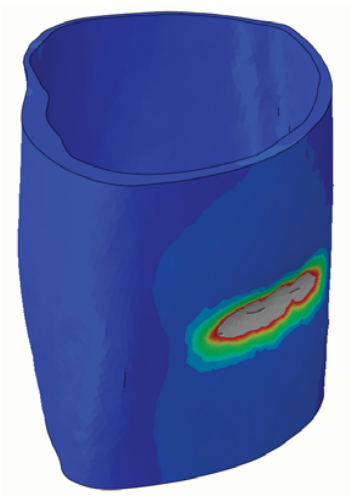

Fig. 12 Contour plot of the fat tissue from the lumped FE model showing the von Mises effective stress

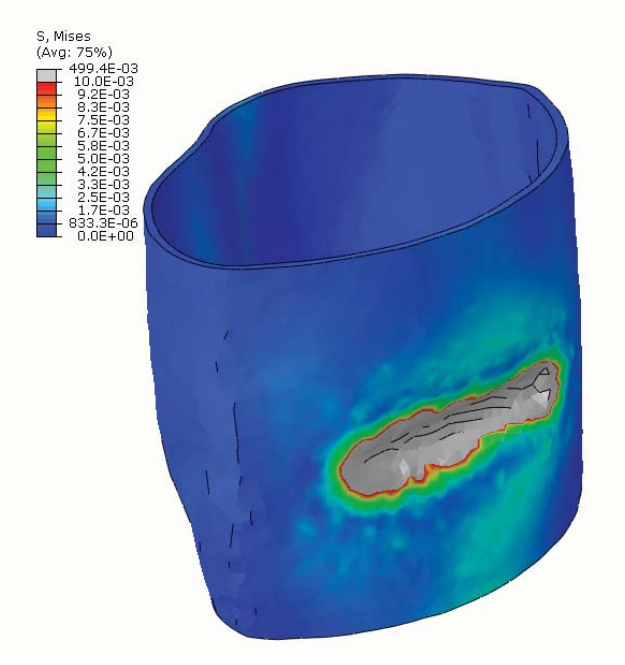

Fig. 13 Contour plot of the skin tissue from the detailed FE model showing the von Mises effective stress

Fig. 14 Contour plot of the skin tissue from the lumped FE model showing the von Mises effective stress

D. Skin

The skin tissue underneath the cylinder is thin and the deformation is virtually transmitted directly to the fat tissue it becomes incompressible even at low loads. Again, the skin tissue is thin and it will follow the deformation of the fat tissue. Here, the speckle pattern that is observed in Figs. 11 and 13 is even more prominent. Following the argument stated previously, this is due to, now, three soft materials stacked after one another. This is not observed for the lumped model seen in Fig. 14.

IV. Discussion

It is not surprising that bi-material interfaces will induce differences in stress. Nevertheless, the aim of the present study is to reveal how a detailed model can highlight where these differences occur. It has been established in literature that sharp bony prominence areas have a major impact on the development of pressure ulcers and deep tissue injuries. However, in the detailed FE model it is observed that the softer regions of the lower limb in fact induces shear strains that might reduce blood flow to certain regions. Thus, the cells in these regions will eventually be subject to hypoxia or even

necrosis. This type of analysis is not possible with the lumped FE model since the material is isotropic without any 'internal' borders, which is clearly seen in Fig. 6 where the stress field is quite smooth.

V. Conclusions

In this study it has been shown that a detailed finite element model is necessary in order to analyze the internal mechanical strains that might lead to pressure ulcers or deep tissue injury. It should be noted that lumped FE models can yield the same load vs. displacement curves as a detailed FE model. However, this is without highlighting the internal strains to the degree that conclusions can be made about the internal conditions for individual tissues.

For realistic prediction of contact stresses and internal mechanical conditions, a FE model must incorporate accurate material models and boundary conditions. This work has attempted to highlight some of the basic requirements needed to study the internal mechanical conditions for different soft human tissues.

Acknowledgment

The authors would like to thank the Region Jönköpings län and Jönköping University for funding the research. The authors would also like to thank Hotswap Norden, Ottobock Scandinavia and Össur Nordic for funding and collaboration.

References

[1] J. Black, M. M. Baharestani, J. Cuddigan, B. Dorner, L. Edsberg, D. Langemo, *National Pressure Ulcer Advisory Panel's updated pressure ulcer staging system*, Advances In Skin & Wound Care, vol. 20, pp. 269-274, 2007.

[2] E. Linder-Ganz, N. Shabshin, Y. Itzchak, and A. Gefen, *Assessment of mechanical conditions in sub-dermal tissues during sitting: a combined experimental-MRI and finite element approach*, Journal Of Biomechanics, vol. 40, pp. 1443-1454, 2007.

[3] X. H. Jia, M. Zhang, and W. C. C. Lee, *Load transfer mechanics between trans-tibial prosthetic socket and residual limb - dynamic effects*, Journal of Biomechanics, vol. 37, pp. 1371-1377, 2004.

[4] S. Portnoy, I. Siev-Ner, N. Shabshin, A. Kristal, Z. Yizhar, and A. Gefen, *Patient-specific analyses of deep tissue loads post transtibial amputation in residual limbs of multiple prosthetic users*, Journal of Biomechanics, vol. 42, pp. 2686-2693, 2009.

[5] D. Lacroix and J. F. R. Patino, *Finite Element Analysis of Donning Procedure of a Prosthetic Transfemoral Socket*, Annals of Biomedical Engineering, vol. 39, pp. 2972-2983, 2011.

[6] A. Hadid, N. Belzer, N. Shabshin, G. Zeilig, A. Gefen, and Y. Epstein, *The effect of mechanical strains in soft tissues of the shoulder during load carriage*, Journal of Biomechanics, vol. 48, pp. 4160-4165, 2015.

[7] A. J. Narracott, G. W. John, R. J. Morris, J. P. Woodcock, D. R. Hose, and P. V. Lawford, *A Validated Model of Calf Compression and Deep Vessel Collapse During External Cuff Inflation*, IEEE Transactions on Biomedical Engineering, vol. 56, pp. 273-280, 2009.

[8] P. Y. Rohan, P. Badel, B. Lun, D. Rastel, and S. Avril, *Prediction of the Biomechanical Effects of Compression Therapy on Deep Veins Using Finite Element Modelling*, Annals of Biomedical Engineering, vol. 43, pp. 314-324, 2015.

[9] J. S. Affagard, P. Feissel, and S. F. Bensamoun, *Identification of hyperelastic properties of passive thigh muscle under compression with an inverse method from a displacement field measurement*, Journal of Biomechanics, vol. 48, pp. 4081-4086, Nov 2015.

[10] R. B. Groves, S. A. Coulman, J. C. Birchall, and S. L. Evans, *An anisotropic, hyperelastic model for skin: Experimental measurements, finite element modelling and identification of parameters for human and murine skin*, Journal of the Mechanical Behavior of Biomedical Materials, vol. 18, pp. 167-180, 2013.

[11] C. Then, J. Menger, G. Benderoth, M. Alizadeh, T. J. Vogl, F. Hübner, *Analysis of mechanical interaction between human gluteal soft tissue and body supports*, Technology And Health Care: Official Journal Of The European Society For Engineering And Medicine, vol. 16, pp. 61-76, 2008.

[12] H.Y. Cheng, C.L. Lin, H.W. Wang, S.W. Chou *Finite element analysis of plantar fascia under stretch - the relative contribution of windlass mechanism and achilles tendon force.*, Journal of Biomechanics, vol. 41(9), pp. 1937-1944, 2008.

[13] S. Evans, C. Holt *Measuring the mechanical properties of human skin* in vivo *using digital image correlation and finite element modeling.*, Journal of Strain Analysis for Engineering Design, vol. 44(5), pp. 337-345, 2009.

[14] B. Hoffmeister, S. Smith, S. Handley, J. Rho *Anisotropy of Young's modulus of human tibial cortical bone.*, Medical and Biological Engineering and Computing, vol. 38(3), pp. 333-338, 2000.